JOURNAL OF MATERIALS SCIENCE **40** (2005) 5591–5596

The failure analyses on ZnO varistors used in high tension devices

M. A. RAMÍREZ*
Applied Mineralogy Group (GMA), Faculty of Mines, National University of Colombia, Cra 80 # 68-28, Medellín
E-mail: miganr@kenter.com

P. R. BUENO, W. C. RIBEIRO, J. A. VARELA
Chemistry Institute, UNESP—Paulista State University, C.P. 355, 14801-970, Araraquara, SP Brazil

D. A. BONETT, J. M. VILLA, M. A. MÁRQUEZ, C. R. ROJO
Applied Mineralogy Group (GMA), Faculty of Mines, National University of Colombia, Cra 80 # 68-28, Medellín

Published online: 25 August 2005

The main purpose of this work is to evaluate the failure caused by electrical discharge on commercial ZnO varistor doped with oxide of Bi, Sb, Si, Cr, Co utilized in electric transmission systems. In order to observe the effect of electrical discharge over the microstructure and electrical properties of the varistors, two kinds of pulses were applied: long pulse (2000 ms) and short pulse (8/20 μs). In both cases, a decrease in grain size and increase in micropores and leakage current were observed. The degraded samples present oxygen defficiency mainly in the grain boundary and phase tranformation from the bismuth oxide phase. © *2005 Springer Science + Business Media, Inc.*

1. Introduction

Zinc oxide varistor is a ceramic device with non-ohmic behavior which allows the protection of electrical equipment against the surge. The nonlinear characteristics are attributed to the formation of double Schottky barriers at the zinc oxide grain boundaries [1]. This nonlinearity makes them suitable for clamping the voltage to an acceptable level when a high voltage surge comes to transmission equipment due to switching operations or lightning [2]. The particular interest of the ZnO varistors is the properties related to the current-voltage range in which the materials can be used [3]. The first development in ZnO varistor was performed in Japan by Matsuoka toward 1970, where different kinds of additives were tested in order to improve the electrical characteristics. Afterwards, in the 80's decade the importance of dopants on the structural and microstructure of the ceramic varistor besides the role of secundary phases in the grain boundary are well investigated [4, 5]. The behavior of a ceramic varistor is determined by microstructure, grains conduction and grain boundary resistivity [6]. ZnO varistors are made from ZnO doped with various metallic oxide additives, such as Bi_2O_3, Sb_2O_3, CoO and Cr_2O_3. In such materials small amounts of oxides, are added to control the electrical characteristics of the zinc oxide grain boundaries, and thus to optimize the varistor behaviour [7]. The microstructure of the varistor is composed by ZnO main phase, spinel, pyrochlore and a Bi-rich phase. Depending on the processing conditions, the Bi-rich phase may have different structures, such as α, β or δ Bi_2O_3. Such phases exist mainly at ZnO multigrain junctions, and sometimes spinel is embedded in ZnO grains [8]. The grain size in high tension ZnO varistors has been reported in the range 5–30 μm, showing elliptical or hexagonal shape which is affected by chemical composition, sintering temperature and time [9]. The variables used for design the surge arrester is: leakage current, electrical field threshold and absoption energy store [10]. Eda [11] report two typical failure: cracking and puncture while Lengauer *et al.* [12] addresses to the pulse induced fracture, which may occur during standardized screening testing of varistors with high current pulses of very short duration (of fews μs). Several authors [10, 13, 14] found an decrease in density and grain size and an increase in leakage current due to the distortion of the cation distribution after degradation affecting the Schottky barrier. Therefore, the stability of ZnO varistors against constant voltage biases, ac and dc, or surge voltage is recognized as one of the important subjects to be investigated [15]. The varistor has been exposed to different type of stresses such

*Author to whom all correspondence should be addressed.
0022-2461
DOI: 10.1007/s10853-005-1366-4

as normal operating voltage, transient, switching and lightning overvoltages. Depending on the intensity and frequency of the pulses the developed stress may damage the varistor. Considering that few investigations report the effect of current pulses in the microstructure the main purpose of this work is to evaluate the failure caused by electrical discharge on commercial ZnO varistor doped with oxides of Bi, Sb, Si, Cr, Co, Mn utilized in electric transmission systems. By this purpose two kind of pulses were applied: large pulses (2000 ms) and short pulses (8/20 μs).

2. Experimental procedure

In this research (8) lightning arresters with nominal values 10 kV, 10 kA, polymeric haussing with 4 blocks of ZnO varistor were used. Three groups were analyzed: group 1 (lightning arrester free of failure, sample P1), group 2 (lightning arrester degraded by large pulses, samples P3, P4, and P5) and group 3 (lightning arrester degraded by short pulses, samples P2, P6, P7 and P8).

After conditioning the current impulsed generator (CIG) it was necessary to execute the impulses until degradation of the element (high leakage current and change in the wave current pulse and voltage). During the application of each pulse an enough time to cool down the sample to room temperature was used. Latter, one block of the varistor lightning arrester which presents bigger macrostructural degradation was selected. The microstructure analyses was performed by optical microscopy (OM) where the size and shape of the grains were determined. Scanning electron microscopy (SEM) combined to WDS was used to study the type of dopants and their localization. The used equipament was JEOL, JSM-5910LV by looking the surface of a thin polish section. X-ray diffraction (D8 advance Bruker AXS) was used to analyse the mineral phases and establish changes in the lattice parameters. Mercury porosimeter (Pore Sizer 9320 micromeritics) was used to determine the micropores. For electrical properties, silver electrodes with area of 0.496 cm^2 were deposited on both surfaces of the sintered pellets. Current-voltage measurements were taken using a high voltage unit (KEITHLEY Model 237), while impedance spectroscopy was taken using a frequency response analyzer (HP 4194 A) at frequencies ranging from 100 Hz to 15 MHz, with an amplitude voltage of 1 V. The electrical properties such as nonlinear coefficient α, breakdown field E_r, barrier voltage V_b were calculated from E vs. J results while the barrier height ϕ_b was calculated from the results of impedance spectroscopy.

3. Results and discussion

Fig. 1a shows the behavior of lightning arrester at different current pulses until failure. It is observed an increase in the current and abrupt decrease in the voltage due to the change of varistor behaviour caused by physical failures (cracking and puncture). Fig. 1b and c presents the time dependence of current and voltage after application of current pulses. It was verified that the wave shape changes, that is, current increase and voltage decrease between the first an last pulse.

Table I illustrates the electrical properties for standard and degraded samples. The electrical parameters were calculated from E vs. J plot. The degradation process leads to an increase in the leakage current; consequently, there is an expected decreasing in the nonlinear coefficient. Therefore, after degradation process the electrical properties are strongly affected by the chemical changes in the grain boundary. The same behavior was observed for the samples degraded with long pulses so that presenting a decrease in the nonlinear coefficient and an increase in the leakage current. Table I also presents the barrier height calculated by the thermionic approach and complex plane analysis at constant frequencies, which is equivalent to C-V measurements. As can be seen in Table I, the results differ greatly. The differences can be explained by the fact that for ZnO-based varistor systems the grain-boundary capacitance is frequency dependent [16]. For convenience, in the present work, the grain-boundary capacitances were obtained in 1 MHz fixed frequency which does not eliminates the influence of trapping activity so that influencing the calculation of the barrier height. Although the thermionic model does not takes into account the complexities of the polycrystalline structure, in the present case, the barrier height values calculated using this model better reflects the *dc* nonohmic features. It can be observed an increase in the leakage current after the degradation process. This can be explained by the lower amount of oxygen species in the grain boundary, which affects the electronic transport and consequently the leakage current. It can be clearly

TABLE I Electrical characterization for the standard sample and degraded with different types of pulses

Sample	Nonlinear coefficient α	Breakdown electric field E_r (V/cm)	Leakage current I_f (mA)	Mean grain size (μm)	Barrier voltage V_b (V)	ϕ_b (eV)	β (eV·V$^{-1/2}$·cm$^{-1/2}$)
P1	44.9	2094	0.423	10.62	2.22	0.57 (2.6)*	0.0052
P2	17.5	1893	6.542	10.10	1.91	0.47	0.0064
P3	13.2	2088	28.160	9.71	2.03	0.02 (1.97)*	0.0044
P4	23.7	2150	2.470	10.34	2.22	0.25 (2.41)*	0.0047
P5	21.5	2267	1.574	9.90	2.24	0.41	0.0049
P6	23.3	2055	3.527	9.77	2.00	0.17 (1.78)*	0.0062
P7	16.1	2270	5.000	9.72	2.21	0.34 (2.11)*	0.0061
P8	17.2	2311	9.416	9.44	2.18	0.45	0.0071

*Barrier height calculated by the impedance spectroscopy (C-V).

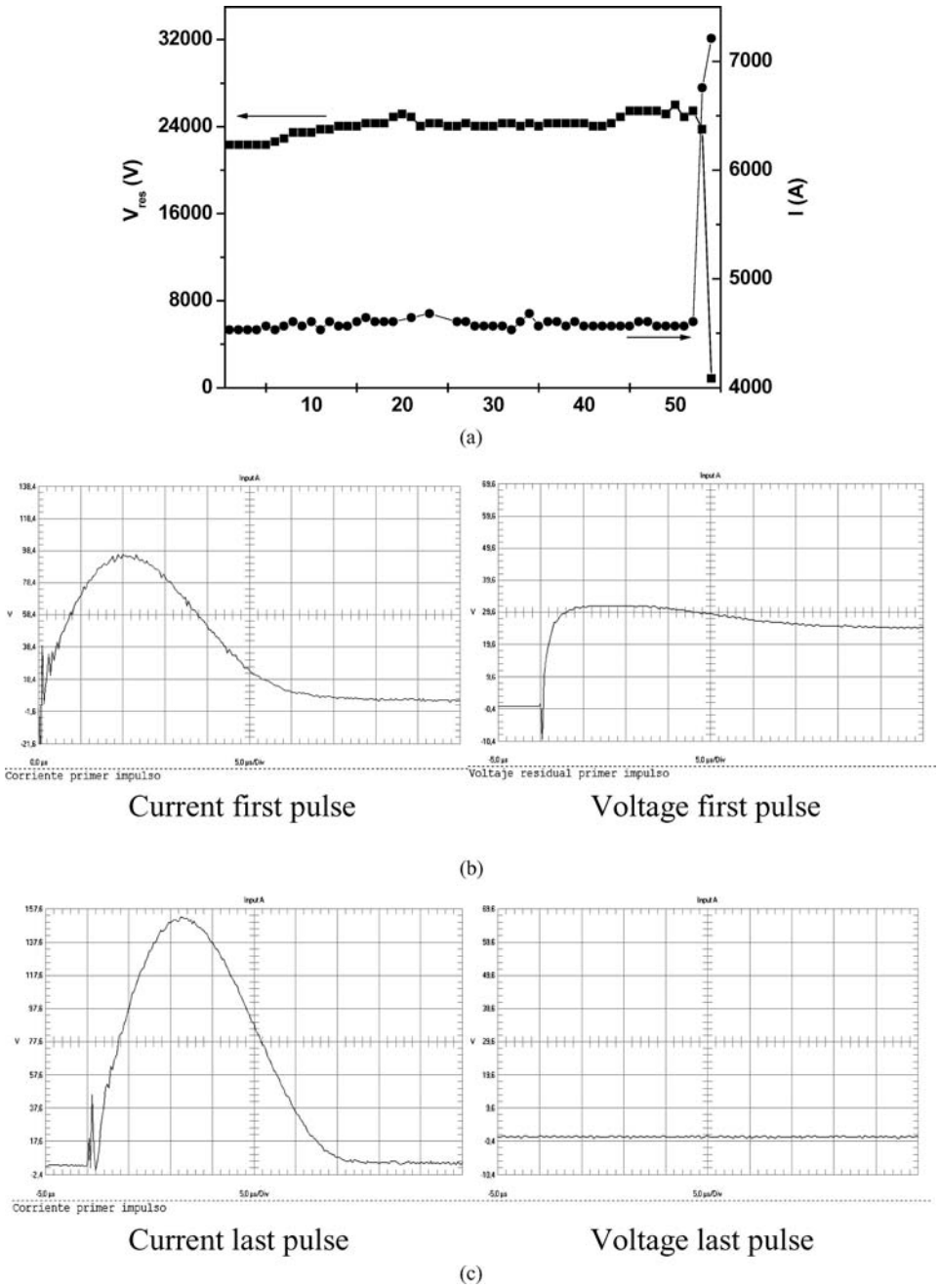

Figure 1 (a) I and V in dependence of number of pulses for degraded sample with short pulses (P2). Current and residual voltage for: (b) First pulse and (c) Last pulse.

seen that after the degradation process a barrier deformation occurs leading to a change in the ϕ and β values. The degradation process can be usually explained by the defect model proposed by Gupta and Carlson [17]. However, our results are in good agreement with the model proposed by Bueno *et al*. [18] and Leite *et al*. [19] for ZnO varistors and for SnO_2 based varistors. In model for ZnO varistors, the Schottky type barrier consists of two components in the depletion layer a stable component consisting of spatially fixed positively charged ions and a metaestable component consisting of mobile zinc interstitials in the depletion layer. Under external stress, zinc interstitials in the depletion layer are driven to migrate toward the grain boundary interface to react with the O_{ads}, and neutral defects are formed at the interface. The barrier height and the width of the depletion layer are thus continually reduced by the decreasing metaestable component through the decreasing concentration of Zn interstitials by diffusion and chemical reaction. As a matter of fact, it has been concluded by some researchers that the common relaxation process is associated with the singly ionized oxygen vacancy, V'_O [20, 21]. The potential barriers have a Schottky-like nature due to negative interfacial states, the selfsame nature often found in all metal oxide varistors and in most metal oxide gas sensors [22] at higher temperatures. Considering such a grain boundary configuration, annealing under a reducing atmosphere (N_2, Ar, or vacuum) eliminates excess oxygen, allowing the metal atoms to remain and, thereby, decreasing the nonlinear electrical properties of the material. The barrier height values obtained by impedance spectroscopy (Table I) are in good agreement with the experimental measurement values obtained by microprobe [8–23].

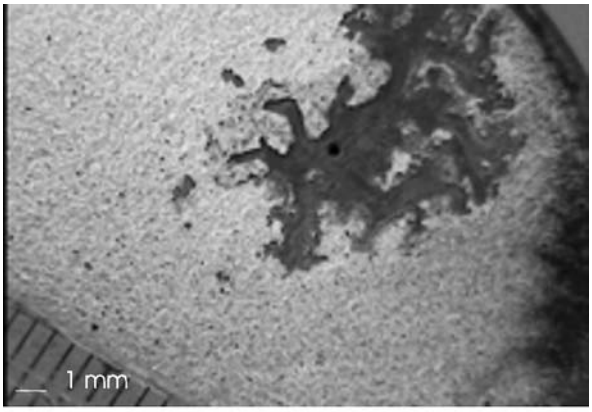

(a)

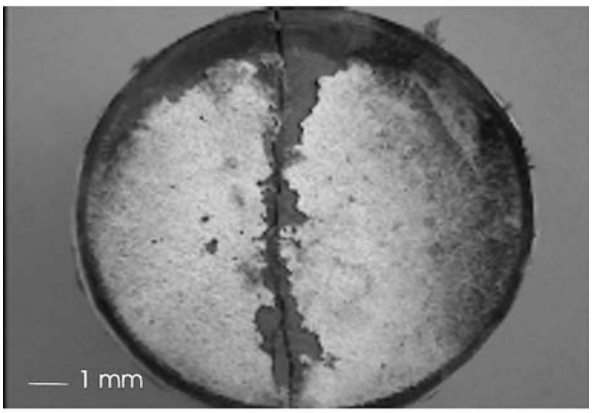

(b)

Figure 2 Images of different failures for samples degraded with long pulses (P5) (a) puncture and (b) cracking.

Fig. 2 shows a photography of the sample degraded with long pulses (P5) which presents macrostructural failure. It can be observed two types of failure (puncture—Fig. 2a) and (cracking—Fig. 2b). These phenomena occur due to the excessive overheating of a varistor caused by a repeated lightning or switching current impulses of high magnitude that exceed the thermal capacity of the arrester leading to degradation of its characteristics. The majority of the electrical energy in a current pulse imposed on a varistor is dissipated as heat within it. According to the Eda [11] the puncture mode is observed when the varistors are subject to current pulses ($>50\ \mu s^{-2}$ ms) with current densities $<3{\cdot}10^{-3}$ A cm^{-2}, whereas it was observed in this work that the lightning arrester (P5) submitted to long pulses present two types of failure, puncture and cracking. Other source of physical failure is the presence of microstructural defects as micro-cracks and micro-pores. The nature of these defects has not been identified although they possibly have a origin during the varistor processing [24].

Mercury porosimetry shows an increase in the micropores when the samples were degraded with long and short pulses (Fig. 3) due the increase of temperature produced during the electrical discharge. This leads to the recristallization of the grains in a presence of liquid phase (Bi_2O_3) decreasing the grain size and increasing the porosity.

The porosity also was evaluated by optical microscopy (OM) where is possible to verify a larger

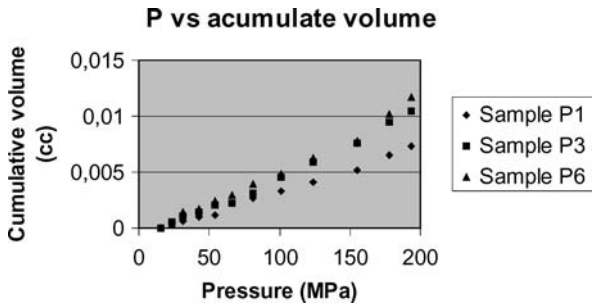

Figure 3 Pressure as a function of accumulate volume for the standard samples (P1) and degraded with short (P6) and long pulses (P3).

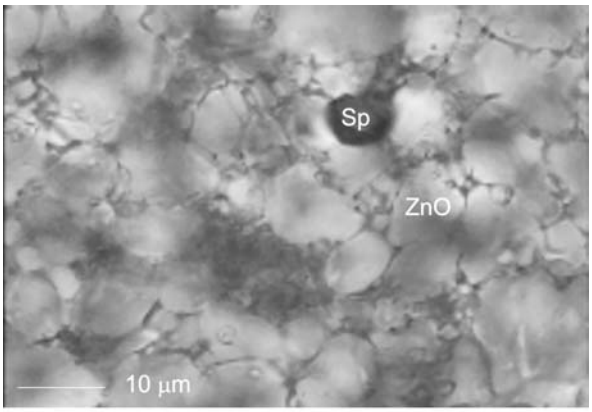

(a)

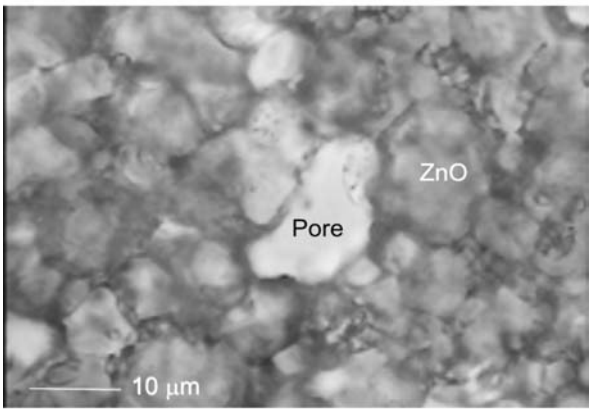

(b)

Figure 4 Optical microscopy of the sample: (a) standard (P1) and (b) degraded with long pulse (P3).

amount of pores in the degraded samples (Fig. 4). It also can be seen the presence of elongated grains although the major part consists of hexagonal grains. The micrograph also shows the presence of a dark region characteristic of the spinel phase and a light region characteristic of the ZnO main phase. A decrease in grain size was noted in samples failure compared with samples free of pulses due to the deformation of the lattice after the application of current pulses. In this case, the intercept method was used to calculated the grain size (Table I). Nan *et al.* [25] suggests that the varistor behavior depends on the contribution of the grain boundaries and the thopological arrangement of the grains. In their work, they assumed that the modifications in grain boundary and in grain size potential reduce the nonlinearity conduction when compared with the microstructure consisting of homogeneous grains.

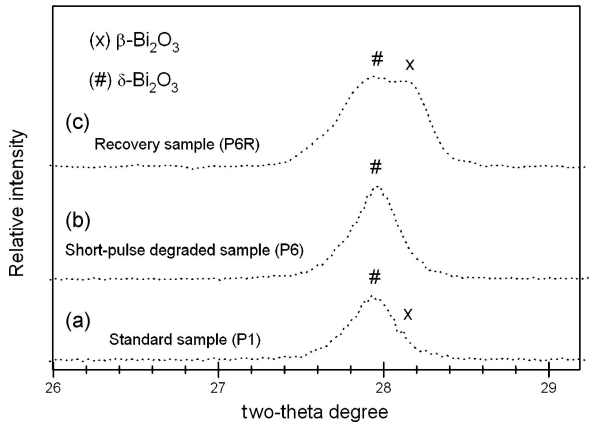

Figure 5 XRD data of the main Bi_2O_3 peak for different varistor conditions: (a) standard (P1), (b) degraded (P6) and (c) recovered (P6R).

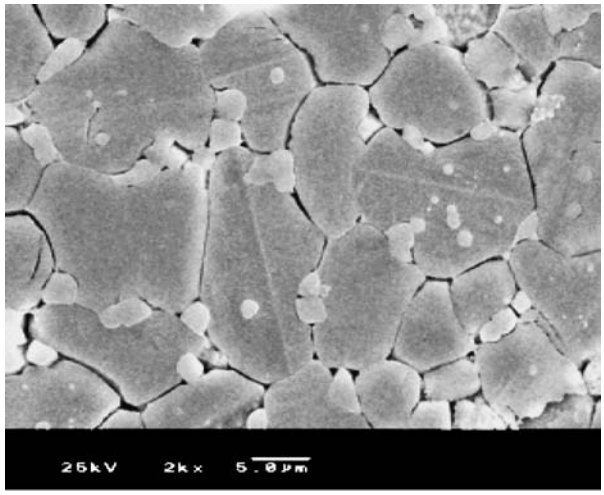

(a)

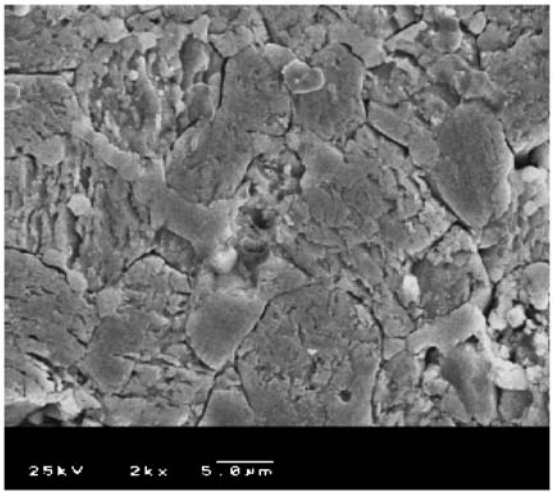

(b)

Figure 6 SEM for the sample: (a) standard (P1) and (b) Degraded with long pulses (P3).

For high-field applications, the microstructural requirements include homogeneous and uniform dopant distribution [26]. The current that can flow along the material is strongly affected by the microstructural disorder since the conductance of the surrounding regions changes. Thus, the effect of microstructural disorder is especially pronounced when it is in direct electrical contact with the electrodes. In an uniform material the presence of elongated grain with a barrier voltage is sufficient to initiate current localization. Besides that, the microstructural inhomogeneities and large grains also can cause current localization. The increase in grain size, for a fixed composition, result in an increase in leakage current and a reduction in the switching voltage. It can be observed that larger grains and lower-grain boundary potential barriers can cause partial short-circuiting enhanced the current effect.

Fig. 5 illustrates the influence of the degradation process on the Bi_2O_3 phase ($2\theta = 28.1^\circ$) present on varistor system with XRD. In the standard sample (P1) two phases are observed δ-Bi_2O_3 and β-Bi_2O_3. After degradation the β-Bi_2O_3 phase disappears and crystallizes the δ-Bi_2O_3 phase (P6). In the recovered sample, there is the re-crystallization of the β-Bi_2O_3 phase while the δ-Bi_2O_3 phase remains constant (P6R). Consequently, one can mention that the recovery is important to re-establish the phases lost during the degradation process. According to the methodology described by Ramírez *et al.* [27], the β-Bi_2O_3 phase can be completely recovered after thermal treatment in oxygen atmosphere. Many researchers have reported the effect caused by the bismuth phases on the microstructure (densification) and on the varistors electrical properties [8, 28]. They observed that due to the high volatility of bismuth rich phases the density of the sample decreases and the leakage current increases after degradation. The role of Bi as the ''grain boundary activator'' may, be limited to supplying excess oxygen to the grain boundaries. The bismuth-rich phase is interconnected and continuous along the three and four grain junctions throughout the microstructure. This microstructure is considered to be crucial for the transport of oxygen into the material during postsintering annealing. Some authors also state that nonohmic properties can be enhanced using ''highly oxygenated'' Bi_2O_3 as a starting material. Consequently, the decrease in the oxygen species is indication of the failure in ZnO varistor decreasing the height of Schottky barriers.

Fig. 6a shows SEM micrography of the standard sample which presents a typical ZnO varistor microstructure. The matrix is composed of grains with size of about 10 μm surrounded by small spynel grains (1 μm) which can be located intra-grains or at grain-boundary region. The stress caused by the degradation process affects the varistor microstructure inhibiting the visualization of some grain boundary area (Fig. 6b). Comparing the SEM/WDS analyses for the degraded and standard samples it was noted an oxygen defficiency (Table II) in the bulk and in the grain boundary for the degraded sample. However, a large deficiency of the oxygen element was found in the grain boundary rather than in the surface of the grain. This causes a decrease of the height barrier affecting the eletrical properties of the varistor. The analyses was performed at different points of the sample showing differences in the chemical potencial between grain volume and the grain boundary. The oxygen deficiency causes difference in resistivities due to a non-equilibrium defect chemistry process, arising during the cooling period. Bueno *et al.* [18] observed that the decrease of oxygen species

TABLE II SEM/WDS analysis of oxygen content in different regions for the standard sample and degraded with different types of pulses

Sample	Region analyses	Oxygen content (counts/second)
P1	Center	50.4
	Boundary	139.7
P3	Center	136.5
	Boundary	112.8
	Twin	122.3
P6	Center	91.6
	Boundary	72.0

results in a change in the voltage-current characteristics of the varistor playing a key role in the grain boundaries of such ceramics. Chemical origins of the potential barrier in polycrystalline ceramics (whatever the n-type semiconductor matrix) depend on the amount of oxygen present at grain boundary interfaces. Earlier reports have also suggested that the varistor characteristics are related to the particular crystalline form that the Bi_2O_3 takes on with oxygen at the grain boundary surface. Several degradation mechanisms have been reported in the literature such as electron trapping, dipole orientation, ion migration that exist in the intragranular and depletion layers and oxygen desorption. The degradation should be promotted by reactions that eliminate the defects formed during sintering. During electrical stressing at high temperatures the varistor would be "energized" possibiliting that enough zinc interticials could react with zinc vacancies at the grain boundary leading to an decrease of the barrier height. When the applied electric field is removed an inverse process would take place and barrier height would be reestablished.

4. Conclusions

In summary, we observed that the degradation caused by the large and short pulses affects the structural and properties of the ZnO varistors. A decrease in grain size was observed due a non-uniform distribution of the energy in the varistor. It was also noted an increase in the leakage current for the samples which present high porosity. The degraded sample shows oxygen defficiency causing a decrease in the height of Schottky barriers. The electric discharges causes a bismuth oxide phase tranformation and a slight displacement of the main peak. The varistor fabricate with uniform grain size and electrodes avoids the concentration of heat which may leads of failure (puncture and cracking types). However, the varistor reported in literature present two classical failure: puncture (in general for long pulses) and cracking (for short pulses), although in our case some samples present both failure.

Acknowledgment

Mastery in Engineering of Materials and Process, DIME, Faculty of Mines and Academic Direction of the National University of Colombia-Sede Medellín by the financial support of this research and the facilities offered by CMDMC-LIEC at the Chemistry Institute-UNESP and Department of Chemistry-UFSCar.

References

1. C. H. LU, N. CHYI, H. W. WONG and W. J. HWANG, *Mat. Chem. Phys.* **62** (2000) 164.
2. M. AKBAR and M. AHMAD, *Elect. Pow. Syst. Res.* **50** (1999) 79.
3. D. BONELL, "Physics Properties of Ceramics: Zinc Oxide Varistor." Available in http://staff.ub.tu-berlin.de with access18 of July 2004.
4. L. M. LEVINSON and H. T. PHILIPP, *Ceram. Bull.* **65** (1986) 639.
5. D. R. CLARKE, *J. Appl. Phys.* **49** (1978) 2407.
6. L. M. LEVINSON and H. T. PHILIPP, *ibid.* **46** (1975) 1332.
7. H. PFEIFFER and K. M. KNOWLES, *J. Europ. Ceram. Soc.* (2004) "in press".
8. E. OLSSON and G. L. DUNLOP, *J. Appl. Phys.* **66**(9) (1989) 4317.
9. K. EDA, *ibid.* **49** (1978) 2964.
10. K. P. MARDIRA, T. K. SAHA and R. A. SUTTON, *IEEE* **9** (2001) 329.
11. K. EDA, *J. Appl. Phys.* **56** (1984) 2948.
12. M. LENGAUER and D. RUBESA, *J. Eur. Cer. Soc.* **20** (2000) 1017.
13. S. S. KIM, H. G. CHO, T. G. PARK and S. Y. YUNG, *IEEE* **2** (2002) 2212.
14. D. ZHOU, C. ZHANG and S. GONG, *Mat. Sci. Eng.* B **99** (2003) 412.
15. T. K. GUPTA, *J. Am. Ceram. Soc.* **73** (1990) 1817.
16. M. A. ALIM, *J. Appl. Phys*, **78** (1995) 4776.
17. T. K. GUPTA, W. G. CARLSON, M. F. YAN and A. HOUER (eds.), *Adv. In Ceram.* **7** (1983) 30.
18. P. R. BUENO, E. R. LEITE, M. M. OLIVEIRA, M. O. ORLANDI and E. LONGO, *Appl. Phys. Lett.* **79** (2001) 48.
19. E. R. LEITE, J. A. VARELA and E. LONGO, *J. Mat. Sci.* **27** (1991) 5325.
20. J. TANAKA, S. I. HISHITA and H. OKUSHI, *J. Am. Ceram. Soc.* **73** (1990) 1425.
21. Y. SHIM and J. F. CORDARO, *ibid.* **71** (1988) 184.
22. M. EGASHIRA, Y. SHIMIZU, T. TAKAO and S. SAKO, *Sens. Actuat.* B **35** (1996) 36.
23. M. TAO, B. AI, O. DORLANNE and A. LOUBIERE, *J. Appl. Phys.* **61** (1987) 1562.
24. A. VOJTA and D. R. CLARKE, *ibid.* **81** (1997) 985.
25. C.W. NAN and D. R. CLARKE, *J. Am. Ceram. Soc.* **79** (1996) 3185.
26. P. DURÁN, J. TERTAJ and C. MOURE, *ibid.* **86** (2003) 1326.
27. M. A. RAMÍREZ, A. Z. SIMÕES, M. A. MÁRQUEZ, A. A. CAVALHEIRO, E. LONGO and J. A. VARELA, *J. Mater. Sci.* (2004) Submitted.
28. M. ELFWIN, R. OSTERLUND and E. OLSSON, *J. Am. Ceram.* **83**(9) (2000) 2311.

Received 11 January
and accepted 4 April 2005